# Molecular-dynamics study of melting on the shock Hugoniot of Al

Ji-Wook Jeong, In-Ho Lee, and K. J. Chang
*Department of Physics, Korea Advanced Institute of Science and Technology, Taejon 305-701, Korea*
(Received 5 March 1998)

We investigate the Hugoniot melting point of Al using a molecular-dynamics approach based on an embedded-atom method. We calculate the Gibbs free energies of the crystalline and liquid phases as a function of pressure and temperature using the coupling-constant integration method and obtain the melting curve up to 1.6 Mbar, in good agreement with experiments. We also examine the melting properties near zero pressure. The Hugoniot equation of states (EOS) up to 1.8 Mbar is obtained from the Rankine-Hugoniot relation and the isotherms determined for different temperatures. Comparing the melting curve with the Hugoniot EOS's for the solid and liquid phases, the Hugoniot melting is found to begin at 1.2 Mbar and to end at 1.4 Mbar, consistent with shock-wave data. [S0163-1829(99)02301-2]

## I. INTRODUCTION

Recently, molecular-dynamics (MD) simulations have made it possible to observe directly the dynamical aspect of solid-liquid phase transitions with increasing temperature.[1,2] Similar studies were also performed for solid-solid phase transitions under compression.[3] With use of the thermodynamic integration method,[1] which considers a thermodynamically reversible path connecting the real system of interest to a reference system, the temperature and pressure dependences of the Gibbs free energy for each phase can be calculated from MD simulations. This integration technique, which avoids the harmonic-crystal approximation and the calculations of the phonon spectrum, has been successfully used to calculate the melting points of Si, Na, and Al.[2,4,5] For Al, Mei and Davenport reformulated the embedded-atom method (EAM) to study the dynamics of melting and freezing with MD simulations.[2] Their calculations, which were limited to the melting properties near zero pressure, suggested the melting point of 800 K, about 130 K below the measured value. On the other hand, Moriarty and co-workers calculated directly the melting curve of Al under pressure from the Gibbs free energies of the solid and liquid phases.[6] Since their theoretical approach does not rely on MD simulations, it required a lattice-dynamics model for the phonon free energy of the solid and a variational fluid theory with a suitable choice of the reference system for the free energy of the liquid. Shock-compression data for Al exhibited the Hugoniot curve which is very different from the isothermal equation of state. To explain theoretically the Hugoniot melting of Al, Moriarty and co-workers extended their generalized pseudopotential theory to the very high-pressure regime and predicted very successfully the melting pressures on the shock Hugoniot.[6]

In this paper, we perform molecular-dynamics simulations to study the dynamics of melting for Al under pressure using the embedded-atom method. To carry out isobaric molecular-dynamics simulations, we employ a variable-cell-shape molecular dynamics that is invariant with respect to simulation cell choice.[7] We examine the melting properties near zero pressure and estimate the melting point to be 802 K, consistent with previous calculations[2] but about 130 K below the experimental data of 933 K. We extend MD simulations to the pressure regime 1.6 Mbar to determine the melting curve and find the pressure variation of the melting point to be well reproduced. Finally, we examine the solid and liquid Hugoniots, and find the melting to begin at 1.2 Mbar and to end at 1.4 Mbar, in good agreement with previous theoretical calculations and shock-Hugoniot data.[6] Thus, the EAM potential used here is accurate enough to describe both the static and dynamical properties at very high pressures and temperatures, with high computational efficiency.

In Sec. II we describe theoretical methods used for the calculations of the Gibbs free energies for the solid and liquid phases and details of molecular-dynamics simulations. In Sec. III the results of the melting points under pressure and the Hugoniot equation of state are presented and discussions are made. We summarize the results in Sec. IV.

## II. THEORETICAL METHOD

The internal energy of Al is calculated using the embedded-atom method (EAM), which has been successful in describing the structural properties of various transition metals.[8,9] In previous work,[2] the cutoff distance used in calculating the embedding function $F(\rho)$ was set to be $r_c = 1.95\, r_0$, which lies between the third and fourth neighbors of the fcc crystal at zero pressure. For compressed phases under pressure, since the nearest-neighbor distance is shortened, the number of neighboring shells depends on pressure. In our calculations, we employ the same cutoff distance $r_c = 1.95 r_0$ and find that this choice of $r_c$ ensures a proper description of the binding energy in the fcc environment, regardless of the number of neighboring shells in the interaction range.

The Gibbs free energy $G(T,P)$ at temperature $T$ and pressure $P$ is calculated using the coupling-constant integration method.[10] In the solid phase of Al, we need to know $G(T_0,P)$ at a reference temperature $T_0$ and choose the Einstein solid with the potential $W_s$ as the reference system. Then, from standard thermodynamic relations, $G(T,P)$ for the solid phase is expressed as

 

$$G(T,P) = -T\int_{T_0}^{T} \frac{\langle U_{\rm EAM} + PV\rangle_{P,T'}}{T'^2}\,dT' - 3Nk_BT\,\ln\frac{T_0}{T_D} + \frac{T}{T_0}\left[\int_0^1 \left\langle \frac{\delta E_s(\lambda)}{\delta\lambda}\right\rangle_{\lambda,V_0,T_0} d\lambda + PV_0\right], \quad (1)$$

where $U_{\rm EAM}$ is the EAM potential, $\langle \delta E_s(\lambda)/\delta\lambda\rangle_\lambda$ is the ensemble average of $\delta E_s(\lambda)/\delta\lambda$ with $E_s(\lambda)$ defined as $\lambda U_{\rm EAM} + (1-\lambda)W_s$ for the coupling constant $\lambda$ ($0 \leqslant \lambda \leqslant 1$), and $T_D$ is the Debye temperature of Al ($=428$ K).

To calculate the Gibbs free energy of the liquid phase, an intermediate reference system with only repulsive interactions $W_l$ was introduced to avoid the possible liquid-gas phase transition.[1] This reference system is obtained by turning off gradually the attractive part of $U_{\rm EAM}$ at constant volume $V_0 = V(T_0,P)$, followed by a reversible volume expansion process to infinite volume at $T_0$. Using the coupling-constant integration method, the Gibbs free energy of liquid Al is given by

$$G(T,P) = -T\int_{T_0}^{T} \frac{\langle U_{\rm EAM} + PV(T',P)\rangle_{P,T'}}{T'^2}\,dT' + \frac{T}{T_0}\left[\int_0^1 \left\langle \frac{\delta E_l(\lambda)}{\delta\lambda}\right\rangle_{\lambda,V_0,T_0} d\lambda + PV_0\right] + Nk_BT\int_0^{\rho_0}\frac{d\rho}{\rho}\left\langle \frac{P}{\rho k_BT_0} - 1\right\rangle_{\rho,T_0} - Nk_BT\left\{\ln\left(\frac{V_0}{N}\right) + \frac{3}{2}\ln\frac{mk_BT_0}{2\pi\hbar^2} + 1\right\}, \quad (2)$$

where $E_l(\lambda)$ is expressed as $\lambda U_{\rm EAM} + (1-\lambda)W_l$.

In our simulations, we use a Nosé thermostat[11] to control the temperature of the ions, which provides the canonical trajectories for the ionic motions. In isobaric molecular-dynamics simulations, there have been proposed several invariant forms of variable cell shape dynamics.[7,12–14] Here we use the variable-cell-shape technique that employs an invariant Lagrangian under modular transformations and eliminates the dynamical effects associated with volume fluctuations.[7] This simulation method has been useful for studying solid-solid phase transitions under pressure, which require extensive changes in computational cell shape. The equations of motion for the atomic positions, thermostat, and cell edges are integrated simultaneously using the fifth-order predictor-corrector algorithm, with a time step of 84 a.u. ($=2.032$ fs). For each simulation run, we first equilibrate the system for a period of 4000 time steps ($\simeq 8$ ps) and use additional 6000 time steps ($\simeq 12$ ps) to calculate the statistical average for a particular thermodynamic state at $P$ and $T$. For the solid phase at zero pressure, we start from a simple cubic simulation cell containing 256 atoms with periodic boundary conditions, initially arranged in a fcc lattice at $T_0$. We use the output configuration of each run as a starting system for the next run, and vary $T_0$ from 300 to 5000 K as the external pressure increases from 0 to 1.6 Mbar, so that the melting point for each pressure lies in the integration range. For a given pressure, we calculate the statistical average of the enthalpy ($U_{\rm EAM} + PV$) in Eq. (1) by taking a time average of molecular-dynamics simulations at temperature $T$. For temperatures between $T_0$ and $T$ ($=T_0+1000$ K), we choose an interval of 50 K and fit the averaged enthalpies to a second-order polynomial to perform the integration. To calculate the $\lambda$ integrations in Eqs. (1) and (2), we vary gradually the coupling parameter $\lambda$ by 0.1 from 0 to 1 and use a polynomial for fitting. Testing polynomials from fourth-order to ninth-order, we find similar results.

For the liquid phase, we start from a completely melted configuration at very high temperature to avoid the superheated state in the simulation of isobaric heating. The statistical averages of the liquid enthalpy and $U_{\rm EAM} - W_l$ in Eq. (2), which are obtained from MD simulations of isobaric cooling with $T_0 = 1100$ K at zero pressure, are fitted to second- and ninth-order polynomials, respectively, which are the same as those used for the solid phase. As the pressure increases to 1.6 kbar, we increase gradually $T_0$ up to 5500 K. The average of $P/(\rho k_BT_0)$ in the volume expansion process is calculated through constant-volume MD simulations, which use a constant matrix $\mathbf{h}$ formed by $\{\vec{a},\vec{b},\vec{c}\}$ in the Lagrangian formulation, where $\vec{a}$, $\vec{b}$, and $\vec{c}$ represent the cell edges. In this case, we choose 10 $\rho$ points between 0 and $\rho_0$ and use a seventh-order polynomial for fitting, as compared to a fourth-order polynomial in previous work.[2] Here we point out that as pressure increases, the potential $W_l$ suggested by Mei and Davenport[2] becomes more repulsive and gives larger fluctuation errors in MD simulations. Thus, it is difficult to determine accurate melting temperatures at high pressures. Using the potential parameter ($\delta \rightarrow \delta/6$) in $W_l$,[2] which represents weaker repulsive interactions, we are able to reduce fluctuation errors and obtain the melting temperatures for pressures 0–1.6 Mbar, which are numerically stable for polynomials up to seventh order.

We perform MD simulations for a wide range of temperature and pressure and make the isothermal equations of state for various temperatures. If two of the three variables ($P$, $V$, and $T$) are fixed in the $P$-$V$-$T$ diagram, we know the other variable and thereby determine the Hugoniot EOS which satisfies the Rankine-Hugoniot relation. The solid Hugoniot curve is obtained for pressures up to 1.5 Mbar, while for the liquid phase the pressure is increased to 1.8 Mbar. Finally, we are able to predict where the Hugoniot melting occurs, by comparing the melting curve with the Hugoniot EOS for each phase.

## III. RESULTS AND DISCUSSION

Our calculated isothermal equations of state at 0 and 300 K are plotted up to 1.5 Mbar and compared with experimental data in Fig. 1. Since the parameters in the EAM potential used here are determined to reproduce the measured values for the cohesive energy, equilibrium lattice constant, and elastic constants at normal pressure, we expect that the equation of state at zero temperature is in better agreement with the measured one, as compared to finite-temperature isotherms. In fact, we find that our equation of state at zero temperature well reproduce the experimental isotherm,[15] while the calculated isothermal curve at room temperature is slightly underestimated by about 3%, particularly, in the region of high pressures. For pressures up to 0.3 Mbar, the two

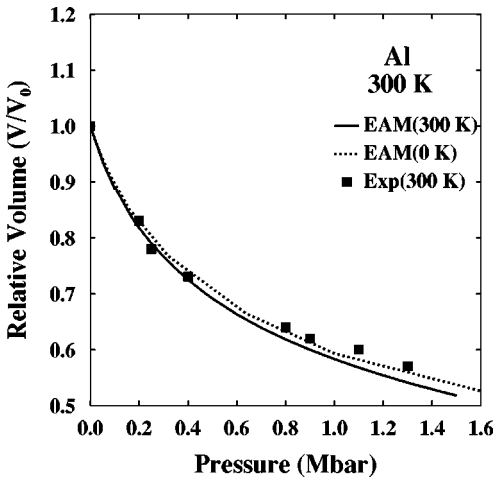


FIG. 1. Isothermal equations of state for Al at 300 K. Filled squares represent experimental data (Ref. 15) and the dotted and solid lines denote the EAM calculations at 0 and 300 K, respectively.

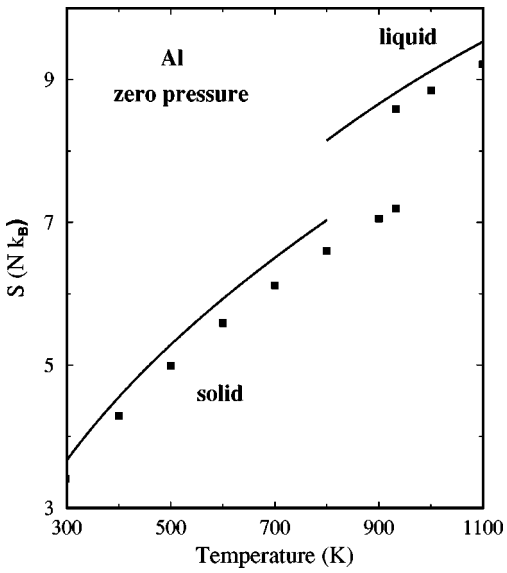


FIG. 2. Calculated entropies of the solid and liquid phases for Al at zero pressure. Filled squares represent experimental data (Ref. 16).

isothermal curves at 0 and 300 K are found to be similar to each other.

We calculate the Gibbs free energies for a wide range of temperature and pressure. At zero pressure, the Gibbs free energy of solid Al at $T_0=300$ K is calculated to be $-3.40$ eV/atom, as compared to the measured value of $-3.43$ eV/atom,[16] whereas for the liquid phase the Gibbs free energy is found to be $-3.87$ eV/atom at $T_0=1100$ K. By finding the equal Gibbs free energies of the solid and liquid phases, we estimate the melting temperature ($T_m$) to be 802 K, in good agreement with the previous EAM results.[2] However, both the calculated values are smaller by about 130 K than the experimentally measured value of 933 K. In Table I, various thermodynamic quantities at the melting point are summarized and compared with other calculations and experiments. The calculated volume of the solid phase is 121.4 a.u., as compared to the experimentally measured value of 120.5 a.u. For the liquid phase, the volume is found to be expanded by 7.1 a.u., while the measured value is 6.5 a.u. In Fig. 2, the calculated entropies of the solid and liquid phases are drawn as a function of temperature at zero pressure and compared with experiments.[16] Since the volume is expanded during phase transition, the liquid phase has softer phonon modes so that the entropy is enhanced. For the solid phase, since our calculated crystal volume is slightly larger than the measured value, the phonon modes seem to be softened, leading to the increase of entropy. In fact, we find that the entropies of the solid phase are overestimated by about 15% and thereby the increase of entropy at $T_m$ is smaller by about 19%. From the change of entropy, the latent heat of transformation is estimated to be about 0.08 eV/atom, consistent with previous calculational results,[2,6] while these calculated values are slightly smaller than the measured value of about 0.11 eV/atom. Nevertheless, overall the temperature variations of entropy for both the solid and liquid phases are in good agreement with experiments. Based on the melting properties near zero pressure, we estimate an initial slope of the melting temperature with respect to pressure, i.e, $dP_m/dT_m=0.15$ kbar/K, which is obtained from the thermodynamic relation known as the Clausius-Clapeyron equation, $dP_m/dT_m=\Delta S_m/\Delta V_m$. Here we point out that the discrepancy between our calculation and the experimental values ($dP_m/dT_m=0.19-0.20$ kbar/K) is reflected by the accumulated errors in $\Delta S_m$ and $\Delta V_m$.

We continue to calculate the Gibbs free energies of the solid and liquid phases so as to construct the melting curve. We perform MD simulations for nine different pressures between 0 and 1.6 Mbar, keeping the same ninth- and seventh-

TABLE I. The melting properties of Al at zero pressure are compared with other EAM and generalized pseudopotential theory (GPT) calculations and experiments. Here $G_m$, $T_m$, $\Delta S_m$, $\Delta V_m$, and $L$ denote the Gibbs free energy, melting point, entropy change, volume change, and latent heat at $T_m$. The volume of the solid phase is given by $V_s$.

| | $G_m$ (eV/atom) | $T_m$ (K) | $\Delta S_m$ ($k_B$) | $V_s$ (a.u.) | $\Delta V_m$ (a.u) | $\Delta V_m/V_s$ | $L$ (eV/atom) | $dP_m/dT_m$ (kbar/K) |
|---|---|---|---|---|---|---|---|---|
| Present EAM | $-3.64$ | 802 | 1.12 | 121.4 | 7.1 | 0.058 | 0.08 | 0.15 |
| Other EAM[a] | $-3.65$ | 800 | 1.17 | | | | 0.08 | |
| GPT[b] | | 1050 | 0.92 | 122.2 | 4.2 | 0.034 | 0.08 | 0.20 |
| Expt.[b] | $-3.73$ | 933 | 1.34–1.39 | 120.5 | 6.5 | 0.054 | 0.11 | 0.19–0.20 |

[a]Reference 2.
[b]Reference 6.

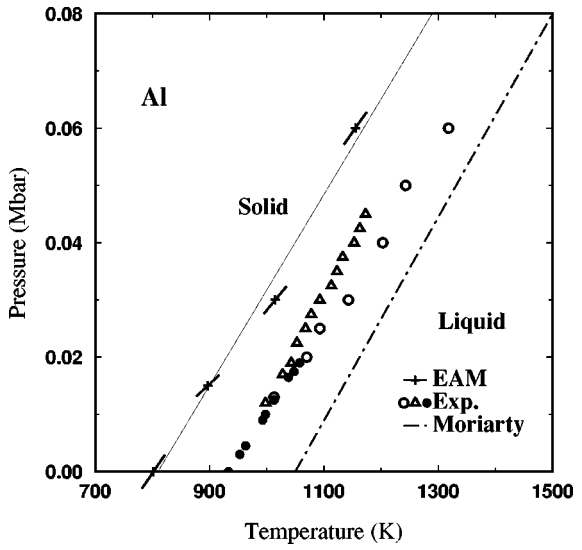


FIG. 3. Calculated melting curve of Al is compared with experiments (Ref. 17) and previous theoretical calculations (Ref. 6). Small line segments on the cross points represent the slopes $dP_m/dT_m$ determined from the Clausius-Clapeyron equation.

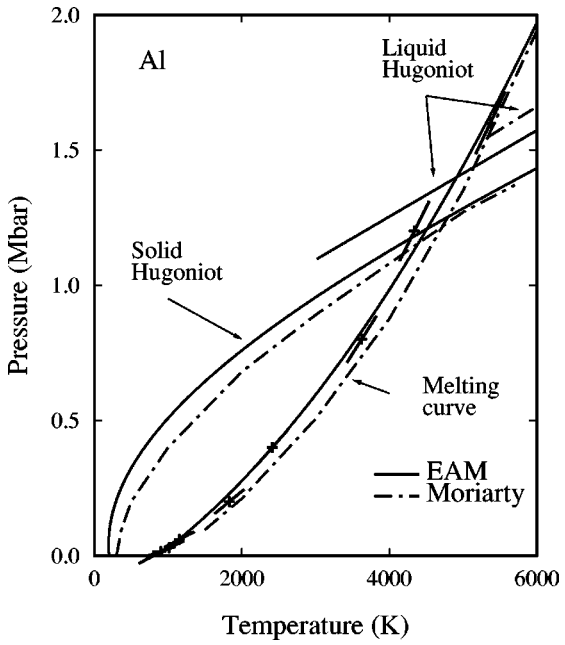


FIG. 4. The solid and liquid Hugoniots of Al are plotted together with the melting curve. The solid and dot-dashed lines represent our EAM calculations and previous theoretical results (Ref. 6), respectively. Small line segments on the cross points represent the slopes $dP_m/dT_m$ determined from the Clausius-Clapeyron equation.

order polynomials for the λ and $\rho$ integrations, respectively, in Eqs. (1) and (2). From the equal-free energy condition, we obtain the melting curve and find the initial pressure variation of the melting temperature $dP_m/dT_m = 0.17$ kbar/K to be in good agreement with both the calculational results from the Clausius-Clapeyron equation and experiments,[6,17] as shown in Fig. 3. In previous calculations,[6] which employ limited information on the structural properties at zero pressure, although the melting point was estimated to be higher by about 120 K, the variation of $P_m$ with temperature agrees well with our calculations. Thus, it is encouraging to employ the EAM potential for determining the melting curve for highly compressed phases. To find the melting curve in the high-pressure region, we choose four different pressures, 0.2, 0.4, 0.8, 1.2, and 1.6 Mbar. Combining with the calculational results for low pressures below 0.06 Mbar, a parabolic fitting gives the melting curve which is in good agreement with previous theoretical calculations,[6] as illustrated in Fig. 4.

It is known that the Rankine-Hugoniot relation gives a proper description of nonequilibrium processes such as explosion and shock compression, while diamond-anvil cells for static high-pressure data. To obtain the theoretical shock Hugoniot, we assume that the nonequilibrium conditions in shock-wave experiments are not very far from thermodynamic equilibrium, so that a particular thermodynamic state is simulated by the molecular-dynamics technique. We perform MD simulations to calculate the isotherm for each pressure, where the pressure ranges from 0 to 1.8 Mbar. Our Hugoniot data up to 0.9 Mbar are given in detail and compared with shock compression data in Table II. The atomic densities during the Hugoniot process are found to be larger by about 3% than the measured values.[18] We note that the temperature determined from the Rankine-Hugoniot relation rises to as high as 3200 K at 0.9 Mbar, while experimentally it was suggested to be about 2800 K.[19] The shock-wave velocity for each dynamic pressure is found to vary linearly with the particle velocity, which was also observed by shock-wave experiments.[18] Considering the thermodynamic equilibrium assumption and the simplicity of the EAM potential, the overall agreement with experiments is encouraging. To determine the melting pressures on the shock Hugoniot, we combine the melting curve and the two Hugoniot data for the solid and liquid phases, as shown in Fig. 4. We find that the melting begins at about 1.2 Mbar and ends at 1.4 Mbar, which are in the range of experimental measurements 1.25–1.5 Mbar. Our results for the Hugoniot melting also agree well with other theoretical calculations,[6] which predicted the pressure range 1.2–1.55 Mbar. In the Hugoniot melting region (see Fig. 4), we note that the liquid Hugoniot is lower by about 0.1 Mbar than that from shock-wave experiments, while the solid Hugoniot is nearly the same with the experimental curve. The discrepancy between the theo-

TABLE II. The calculated Hugoniot data for Al. Here $P_H$, $T_H$, $\rho_H$, and $v_{\text{mass}}$ denote the pressure, temperature, mass density, and mass velocity after shock-wave passage. The shock velocity is given by $v_{\text{shock}}$.

| | $P_H$ (Mbar) | $T_H$ (K) | $\rho_H$ (g/cc) | $v_{\text{shock}}$ (km/s) | $v_{\text{mass}}$ (km/s) |
|---|---|---|---|---|---|
| Calc. | 0.3 | 795 | 3.42 | 7.12 | 1.59 |
| | 0.6 | 1853 | 3.89 | 8.44 | 2.68 |
| | 0.9 | 3239 | 4.22 | 9.57 | 3.54 |
| Expt.[a] | 0.306 | | 3.40 | 7.45 | 1.52 |
| | 0.406 | | 3.54 | 7.96 | 1.89 |
| | 0.603 | | 3.80 | 8.81 | 2.52 |
| | 0.763 | | 3.98 | 9.41 | 2.99 |
| | 0.990 | | 4.19 | 10.17 | 3.59 |

[a]Reference 18.

retical and experimental liquid Hugoniots may be attributed to the fact that the structural information on the liquid state is not included in usual fitting procedures. Nevertheless, a general trend for the solid and liquid Hugoniots agrees well with experiments.

## IV. CONCLUSIONS

We have performed molecular-dynamics simulations to calculate the melting curve of Al up to 1.6 Mbar using the EAM potential, which is determined from the equal-free energies between the solid and liquid phases. The calculated melting properties and the melting curve are in reasonably good agreement with experiments and previous theoretical calculations. From molecular-dynamics simulations and the Rankine-Hugoniot relation, we have also calculated the solid and liquid Hugoniots of Al and find good agreements with previous studies. Based on the results for the melting curve and the Hugoniot curves, we find that melting on the shock Hugoniot begins at about 1.2 Mbar and ends at about 1.4 Mbar. Our calculational results lead us to conclude that the EAM potential used here is accurate enough to describe both the static and dynamic properties, with high computational efficiency.

## ACKNOWLEDGMENT

This work was supported by the ADD.

[1] J. Q. Broughton and X. P. Li, Phys. Rev. B **35**, 9120 (1987).
[2] J. Mei and J. W. Davenport, Phys. Rev. B **46**, 21 (1992).
[3] R. M. Wentzcovitch, Phys. Rev. B **50**, 10 358 (1994); M. Bernasconi, G. Chiarotti, P. Focher, S. Scandolo, E. Tossatti, and M. Parrinello, J. Phys. Chem. Solids **56**, 501 (1995).
[4] O. Sugino and R. Car, Phys. Rev. Lett. **74**, 1823 (1995).
[5] Y. M. Gu, D. M. Bylander, and L. Kleinman, Phys. Rev. B **51**, 15 703 (1995).
[6] J. A. Moriarty, D. A. Young, and M. Ross, Phys. Rev. B **30**, 578 (1984).
[7] R. M. Wentzcovitch, Phys. Rev. B **44**, 2358 (1991).
[8] S. M. Foiles and J. B. Adams, Phys. Rev. B **40**, 5909 (1989), and references therein.
[9] J. Mei, J. W. Davenport, and G. W. Fernando, Phys. Rev. B **43**, 4653 (1991).
[10] *Molecular-Dynamics Simulation of Statistical-Mechanical Systems*, edited by G. Ciccotti and W. G. Hoover (North-Holland, Amsterdam, 1986), pp. 169–178.
[11] S. Nosé, Mol. Phys. **57**, 187 (1986).
[12] M. Parrinello and A. Rahman, J. Appl. Phys. **52**, 7158 (1981).
[13] I. Souza and J. L. Martins, Phys. Rev. B **55**, 8733 (1997).
[14] J. V. Lill and J. Q. Broughton, Phys. Rev. B **46**, 12 068 (1992); **49**, 11 619 (1994).
[15] R. G. Greene, H. Luo, and A. Ruoff, Phys. Rev. Lett. **73**, 2075 (1994).
[16] R. Hultgren, P. D. Desai, D. T. Hawkins, M. Gleiser, K. K. Kelley, and D. D. Wagman, *Selected Values of the Thermodynamic Properties of The Elements* (American Society for Metals, Metals Park, OH, 1973).
[17] J. Lees and B. H. J. Williamson, Nature (London) **208**, 278 (1965).
[18] A. C. Mitchell and W. J. Nellis, J. Appl. Phys. **52**, 3363 (1979).
[19] L. V. Al'tshuler, S. B. Kormer, A. A. Bakanova, and R. F. Trunin, Sov. Phys. JETP **11**, 573 (1960).